Journal of the American College of Cardiology Vol. 54, No. 2, 2009

Published by Elsevier Inc.

ISSN 0735-1097/09/$36.00
doi:10.1016/j.jacc.2009.04.021

Impact of Heterogeneity of Human Peripheral Blood Monocyte Subsets on Myocardial Salvage in Patients With Primary Acute Myocardial Infarction

Hiroto Tsujioka, MD, Toshio Imanishi, MD, PhD, Hideyuki Ikejima, MD, Akio Kuroi, MD, Shigeho Takarada, MD, PhD, Takashi Tanimoto, MD, Hironori Kitabata, MD, Keishi Okochi, MD, Yu Arita, MD, Kohei Ishibashi, MD, Kenichi Komukai, MD, Hideaki Kataiwa, MD, Nobuo Nakamura, MD, Kumiko Hirata, MD, PhD, Atsuhsi Tanaka, MD, PhD, Takashi Akasaka, MD, PhD

Wakayama, Japan

Objectives We examined whether distinct monocyte subsets contribute in specific ways to myocardial salvage in patients with acute myocardial infarction (AMI).

Background Recent studies have shown that monocytes in human peripheral blood are heterogeneous.

Methods We studied 36 patients with primary AMI. Peripheral blood sampling was performed 1, 2, 3, 4, 5, 8, and 12 days after AMI onset. Two monocyte subsets ($CD14^+CD16^-$ and $CD14^+CD16^+$) were measured by flow cytometry. The extent of myocardial salvage 7 days after AMI was evaluated by cardiovascular magnetic resonance imaging as the difference between myocardium at risk (T2-weighted hyperintense lesion) and myocardial necrosis (delayed gadolinium enhancement). Cardiovascular magnetic resonance imaging was also performed 6 months after AMI.

Results Circulating $CD14^+CD16^-$ and $CD14^+CD16^+$ monocytes increased in AMI patients, peaking on days 3 and 5 after onset, respectively. Importantly, the peak levels of $CD14^+CD16^-$ monocytes, but not those of $CD14^+CD16^+$ monocytes, were significantly negatively associated with the extent of myocardial salvage. We also found that the peak levels of $CD14^+CD16^-$ monocytes, but not those of $CD14^+CD16^+$ monocytes, were negatively correlated with recovery of left ventricular ejection fraction 6 months after infarction.

Conclusions The peak levels of $CD14^+CD16^-$ monocytes affect both the extent of myocardial salvage and the recovery of left ventricular function after AMI, indicating that the manipulation of monocyte heterogeneity could be a novel therapeutic target for salvaging ischemic damage. (J Am Coll Cardiol 2009;54:130–8) © 2009 by the American College of Cardiology Foundation

Recent studies have shown that monocytes in human peripheral blood are heterogeneous (1–3). Differential expression of CD14 and CD16 allowed monocytes to be divided into 2 subsets: $CD14^+CD16^-$ and $CD14^+CD16^+$ cells. $CD14^+CD16^-$ cells are often called classic monocytes, because this phenotype resembles the original description of monocytes. Distinct chemokine-receptor expression profiles are also among the phenotypic differences recognized between the subsets: for example, $CD14^+CD16^-$ monocytes expressed C-C motif chemokine receptor 2 (CCR2), whereas $CD14^+CD16^+$ monocytes expressed C-X3-C motif chemokine receptor 1 (CX3CR1) (1–3).

Monocytes and mature macrophages are prominent in the host response to the healing of acute myocardial infarction (AMI). The balance between host defense and repair mechanisms versus the pro-inflammatory properties

See page 139

of the mononuclear phagocyte in injured myocardium should be taken into consideration for therapeutic targeting of monocytes/macrophages (4). In view of the heterogeneity of monocytes, Nahrendorf et al. (5) have shown very recently that distinct monocyte subsets contribute in specific ways to myocardial ischemic injury in mouse myocardial infarction (MI), which led us to

From the Department of Cardiovascular Medicine, Wakayama Medical University, Wakayama, Japan. This work was supported in part by grants from the Ministry of Education, Culture, Sports, Science and Technology, Japan (no. 20590835).

Manuscript received December 27, 2008; revised manuscript received April 9, 2009, accepted April 14, 2009.

explore the relevance of monocyte heterogeneity after AMI in humans.

With the advent of delayed-enhancement cardiac magnetic resonance (CMR) imaging, it is now possible to accurately quantify the extent of myocardial necrosis in vivo (6). It has also been reported that CMR imaging can demonstrate the myocardial area at risk, which shows high signal intensity on T2-weighted images as a result of edema in a canine model of reperfused infarction (7). Therefore, it is clinically feasible to noninvasively evaluate the extent of myocardial salvage by CMR imaging as the difference between myocardium at risk and myocardial necrosis (8,9). In fact, a very recent investigation showed that the myocardial area at risk can be visualized using T2-weighted CMR in patients with AMI (8). The aim of this study was to examine whether distinct monocyte subsets contribute in specific ways to myocardial salvage in patients with AMI.

Methods

The study protocol was approved by the institutional ethics committee of Wakayama Medical University (#2008-535), and written informed consent was obtained from either the patients or their family members.

Patient populations. We enrolled 36 primary AMI patients, 24 unstable angina pectoris (UAP) patients, and 20 stable angina pectoris (SAP) patients when they fitted AMI, UAP, or SAP diagnostic criteria as follows. AMI was diagnosed under the following conditions: 1) when patients experienced chest pain within 24 h before admission that lasted for >30 min and was not relieved by sublingual nitroglycerin; 2) when patients showed ST-segment elevation and/or abnormal Q-wave on an electrocardiogram; and 3) when patients showed elevated serum creatine kinase (CK) levels. Exclusion criteria were as follows: 1) AMI for >24 h from onset; 2) a history of renal dysfunction requiring dialysis; 3) evidence of malignant disease; or 4) unwillingness to participate. All patients received coronary angiography on admission and then underwent emergent percutaneous coronary intervention (PCI) using coronary stents. All patients were routinely treated with heparin, isosorbide dinitrate, ticlopidine, aspirin, and an angiotensin-converting enzyme inhibitor or angiotensin II receptor blocker. Unstable angina pectoris was defined as having ischemic chest pain at rest within the preceding 48 h, transient ST-T–segment depression, and/or T-wave inversion but no evidence of myocardial necrosis by enzymatic criteria. Stable angina pectoris was defined as having effort angina >3 months and a positive exercise test. The diagnosis of coronary artery disease was confirmed by coronary angiography.

Clinical parameters. The clinical parameters assessed included age, sex, and coronary risk factors (smoking, hypertension, diabetes mellitus, hyperlipidemia, and obesity). The diagnostic criteria for coronary risk factors were as follows: hypertension, blood pressure ≥140/90 mm Hg, and/or a history of taking antihypertensive medication; diabetes mellitus, fasting plasma glucose ≥126 mg/dl, casual plasma glucose ≥200 mg/dl, or a diabetic pattern in 75-g oral glucose tolerance test; hyperlipidemia, serum total cholesterol levels >220 mg/dl, or serum triglyceride levels >150 mg/dl; obesity, body mass index ≥25 kg/m^2. Peak CK, peak CK-myocardial band, and left ventricular ejection fraction (LVEF) were selected for analysis as indicators of MI severity.

Abbreviations and Acronyms

AMI = acute myocardial infarction
CK = creatine kinase
CMR = cardiac magnetic resonance
CRP = C-reactive protein
LE = late enhancement
LV = left ventricle
LVEF = left ventricular ejection fraction
MI = myocardial infarction
MRI = magnetic resonance imaging
PCI = percutaneous coronary intervention
PlGF = placental growth factor
SAP = stable angina pectoris
UAP = unstable angina pectoris

Cytometric analysis. For cytometric analysis, monoclonal antibodies against CD14 (fluorescein isothiocyanate [FITC] or phycoerythrin [PE], Clone M5E2, BD Bioscience, San Jose, California), CD16 (PE-Cy^{TM5}, Clone 3G8, BD Bioscience), CCR2 (PE, catalog number FAB151P, R&D Systems Inc., Minneapolis, Minnesota), and CX3CR1 (FITC, Clone 2A9-1, MBL, Nagoya, Japan) were used. Whole blood (100 μl) was incubated with saturating amounts of antibodies for 15 min at room temperature in the dark. For erythrocyte lysis and leukocyte fixation, 1 ml lysing solution was added (BD FACS Lyse, Becton Dickinson, Heidelberg, Germany).

Cytometric analysis was performed in a fluorescence-activated cell scanner (Becton Dickinson) using Cell Quest Software Systems (Becton Dickinson). Monocytes were first gated in a forward scatter/sideward scatter dot plot, and then 3-color fluorescence was measured within the monocyte gate (Fig. 1A). The CD14$^+$CD16$^-$ cells were defined as monocytes expressing CD14, but not CD16 (Fig. 1B, lower right quadrant). Thereafter, CD14$^+$CD16$^-$CCR2 cells were determined (Fig. 1C). The CD14$^+$CD16$^+$ cells were defined as monocytes expressing CD16 and either high levels of CD14 (CD14^{bright}CD16$^+$) (Fig. 1B, upper right quadrant) or lower levels of CD14 (CD14^{dim}CD16$^+$) (Fig. 1B, upper left quadrant). Thus, CD14^{bright}CD16$^+$ and CD14^{dim}CD16$^+$ were not analyzed separately, according to previous studies (10). Thereafter, CD14$^+$CD16$^+$CX3CR1 cells were determined (Fig. 1C).

Blood sampling and analysis. In AMI patients, peripheral blood samples were collected from all subjects as soon as possible after admission and on days 2, 3, 4, 5, 8, and 12 after the onset of AMI. For UAP patients, peripheral blood samples were collected from all subjects as soon as possible and on days 2 and 3 after admission. For SAP patients, peripheral blood samples were collected from all subjects on admission because of planned PCI. The whole blood

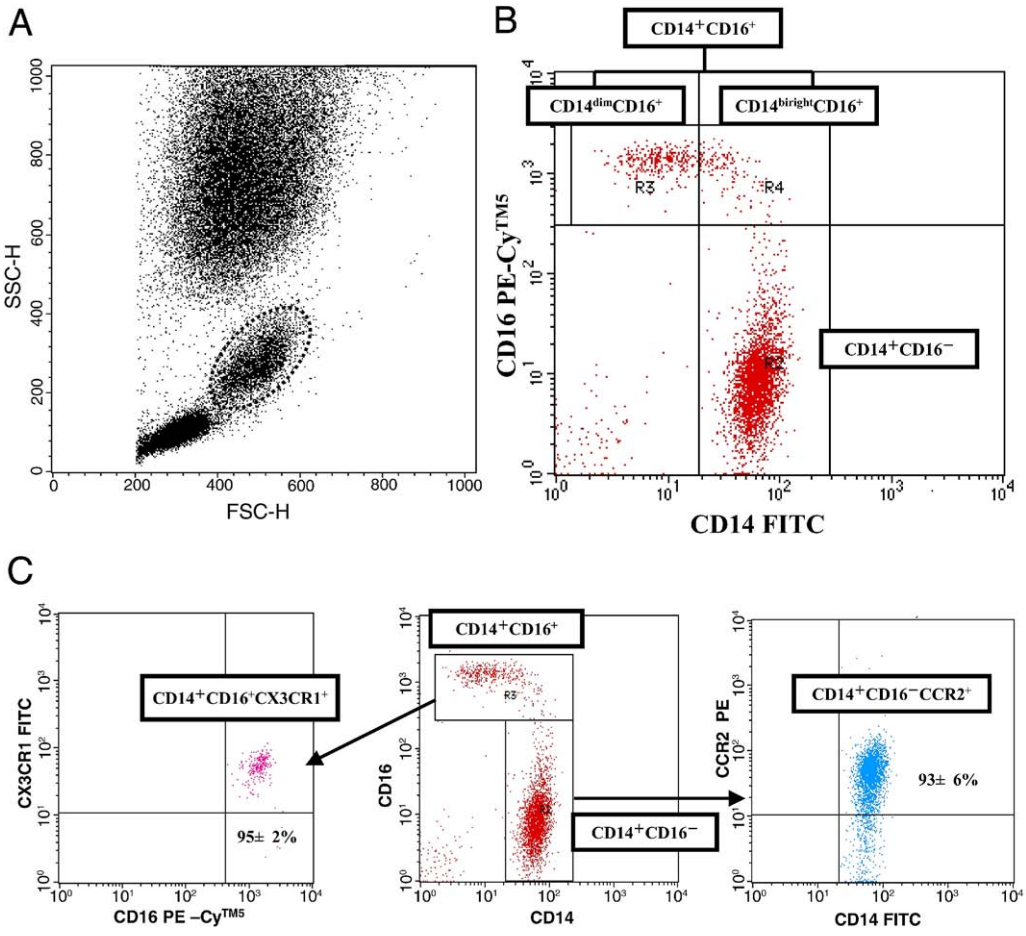

Figure 1 **Fluorescence-Activated Cell Scanner Analysis**

(A) Monocytes were gated in a forward scatter (FSC)/sideward scatter (SSC) dot plot. **(B)** The $CD14^+CD16^-$ cells were defined as monocytes expressing CD14, but not CD16 **(lower right quadrant)**. The $CD14^+CD16^+$ cells were defined as monocytes expressing CD16 and either high levels of CD14 (**upper right quadrant**; $CD14^{bright}CD16^+$) or lower levels of CD14 (**upper left quadrant**; $CD14^{dim}CD16^+$). **(C)** For determination of $CD14^+CD16^+CX3CR1^+$ and $CD14^+CD16^-CCR2^+$ monocytes, 3-color fluorescence (phycoerythrin [PE]-conjugated CD14 antibody [Ab], PE-Cy^{TM5}-conjugated CD16 Ab, and fluorescein isothiocyanate [FITC]-conjugated CX3CR1 Ab) was performed after $CD14^+CD16^+$ cells and $CD14^+CD16^-$ cells were gated **(middle panel)**, $CD14^+CD16^+CX3CR1^+$ cells and $CD14^+CD16^-CCR2^+$ cells were measured, respectively. The $CD14^+CD16^+$ monocytes consisted of 95 ± 2% $CX3CR1^+$ cells **(left)**. Three-color fluorescence (FITC-conjugated CD14 Ab, PE-Cy^{TM5}-conjugated CD16 Ab, and PE-conjugated CCR2 Ab) was performed to determine $CD14^+CD16^-CCR2^+$ monocytes. The $CD14^+CD16^-$ monocytes consisted of 93 ± 6% $CCR2^+$ cells **(right)**. H = height.

samples obtained from all subjects were used immediately for flow cytometry. We also collected plasma samples in ethylenediamine tetraacetate anticoagulant tubes and stored them at −80°C until assayed.

Plasma levels of placental growth factor (PlGF) were measured using commercially available enzyme-linked immunoadsorbent assay kits (DY264, R&D Systems). High-sensitivity C-reactive protein (CRP) was analyzed using a commercially available testing kit (N-Latex CRP II, Dade Behring GmbH, Marburg, Germany).

Noninvasive CMR imaging protocol. The CMR imaging studies were performed using a 1.5-T clinical scanner (Intera Achieva, Philips Medical Systems, Best, the Netherlands) 7 days after the AMI onset, as previously described (8,9). Patients were continuously monitored during the examination using single-lead electrocardiography, repeated blood pressure measurements, and pulse oximetry. With the patient in the supine position, contiguous short-axis cine images covering the left ventricle (LV) from base to apex were acquired using a standard steady-state free-precession sequence. We then applied a breath-hold short-TI inversion recovery pulse sequence (repetition time: 2 R-R intervals; echo time: 90 ms; slice thickness: 8 mm; field of view: 35 μm; matrix: 256 × 512) in 3 short-axis slices (basal, midventricular, and apical) using a body coil. Each slice was obtained during an end-expiratory breath-hold of 12 to 15 s, depending on the patient's heart rate.

We then acquired late enhancement (LE) images in the slice location with the maximum extent of T2 signal abnormality 10 to 15 min after intravenous injection of 0.1 mmol/kg gadolinium-diethylenetriamine penta-acid (Magnevist, Schering, Berlin, Germany). We used a 3-dimensional inversion-

recovery turbo-gradient echo sequence, and images were obtained during an end-expiratory breath-hold. We optimized the inversion time (200 to 300 ms) to null the normal myocardium. The slice positions for both T2-weighted and LE acquisitions matched those of the cine images. There were no complications related to the CMR procedures, and all patients tolerated the procedure well.

CMR imaging data analysis. All analyses were performed by consensus of 2 blinded observers (H.I. and A.K.) on an off-line workstation (View Forum, Philips Medical Systems, Eindhoven, the Netherlands). Epicardial and endocardial borders were traced in each cine image to obtain LV end-diastolic volume, LV end-systolic volume, and left ventricular ejection fraction (LVEF).

The extent of the area at risk (T2-weighted hyperintense lesion) and myocardial necrosis (delayed gadolinium enhancement) were quantified on the same slice location with the maximum extent of T2 signal abnormality (Fig. 2). Percent salvaged myocardium was obtained as follows: 100 × extent of salvaged myocardium/extent of the myocardial area at risk.

Statistics. If not stated otherwise, data are expressed as mean ± SD. Because $CD14^+CD16^-$ and $CD14^+CD16^+$ monocytes were not normally distributed (according to the Shapiro-Wilks test), they were expressed as median and range and analyzed with nonparametric methods. The nonparametric Mann-Whitney *U* statistic was used to test for differences between 2 groups. When >2 groups of subjects were compared, the nonparametric Kruskal-Wallis test was used. If a significant difference was found, pairwise comparisons by Bonferroni test were performed for multiple analyses. Categorical data were given as percentages and were compared by chi-square test. To assess correlations between 2 parameters, simple linear regressions were calculated using the least squares method. Values of $p < 0.05$ were considered significant. All statistical analyses were performed using the statistical software package SPSS version 11.0 (SPSS Inc., Chicago, Illinois).

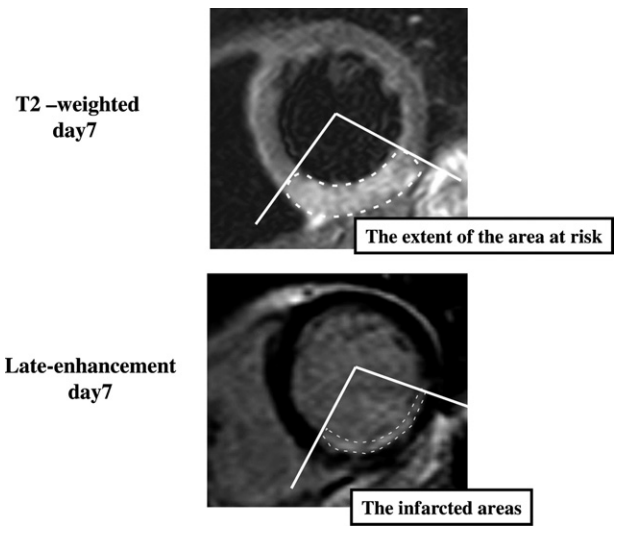

Figure 2 Cardiac Magnetic Resonance Imaging

Measurement of myocardial salvage index evaluated from cardiac magnetic resonance short-axis images obtained 7 days after acute myocardial infarction. In the T2-weighted, fast spin-echo images, the hyperintense areas indicate the extent of the area at risk **(top)**. Late enhancement bright images show the infarcted areas **(lower bottom)**. Percent salvaged myocardium was obtained as follows: 100 × extent of salvaged myocardium/extent of the myocardial area at risk.

Results

Patient characteristics. The characteristics of the study population are summarized in Table 1. The clinical characteristics did not significantly differ among the 3 groups. In AMI patients, there were 27 men and 9 women with a mean age of 69 ± 15 years (range 36 to 85 years). The mean interval from AMI onset to reperfusion was 4.3 ± 3.4 h. The mean value of the maximum CK levels was 1,942 ± 1,892 IU/l, and the mean LVEF during the acute phase was 48 ± 17%. Both total white blood cell and neutrophil counts were elevated at admission, and thereafter decreased (data not shown). The peak monocyte count was 679 ± 259/mm^3 (Table 1). Both peak monocyte and peak monocyte subset counts after AMI did not significantly differ among several parameters of patient characteristics (Table 2).

Natural profile of monocyte subsets levels in CAD. Peripheral whole-blood samples to analyze 2 distinct monocyte subsets ($CD14^+CD16^-$ and $CD14^+CD16^+$) were obtained from patients with UAP and AMI as soon as possible after admission (day 1) and from patients with SAP on hospital day (day 1) as a control. There were not any significant differences in circulating $CD14^+CD16^-$ monocytes among the 3 groups (Fig. 3A). Conversely, circulating $CD14^+CD16^+$ monocytes were significantly decreased in patients with AMI compared with those in UAP or SAP patients (Fig. 3B). In line with previous studies (1–3), $CD14^+CD16^-$ and $CD14^+CD16^+$ monocytes consisted of 93 ± 6% $CCR2^+$ cells and 95 ± 2% $CX3CR1^+$ cells, respectively, in our study population (Fig. 1C). The $CD14^+CD16^-$ and $CD14^+CD16^+$ monocytes selectively express CCR2 and CX3CR1, respectively (data not shown).

Time courses in circulating monocyte subsets levels after AMI. When we conducted measurements in peripheral whole blood obtained on days 1, 2, 3, 4, 5, 8, and 12 after AMI onset, 2 distinct monocyte subsets were mobilized in specific ways after AMI. Circulating $CD14^+CD16^-$ monocytes increased in AMI patients, peaking on day 2.6 ± 0.8 after onset (Fig. 4B). Although circulating $CD14^+CD16^+$ monocytes also increased in AMI patients, peaking on day 4.8 ± 2.9 after onset, no significant change occurred during the 12 days after the peak (Fig. 4C). However, we found that individual peak values of $CD14^+CD16^+$ monocytes were significantly higher in patients with AMI than in patients with SAP (Fig. 4D). Next, we examined whether

Table 1 Patient Characteristics

Characteristic	AMI (n = 36)	UAP (n = 24)	SAP (n = 20)	p Value
Age, yrs	69 ± 15	65 ± 12	67 ± 11	0.31
Sex, male/female	27/9	17/7	12/8	—
Serum creatinine, mg/dl	0.97 ± 0.27	0.82 ± 0.28	0.84 ± 027	0.62
Systolic blood pressure, mm Hg	142 ± 23	139 ± 26	145 ± 17	0.77
Diastolic blood pressure, mm Hg	83 ± 12	80 ± 16	82 ± 16	0.76
Culprit lesion				
LAD	20 (56)	13 (54)	9 (45)	0.61
LCX	5 (14)	3 (13)	5 (25)	0.47
RCA	11 (31)	8 (32)	6 (30)	0.97
Coronary risk factor				
Diabetes mellitus	9 (25)	8 (33)	6 (30)	0.96
Hypertension	19 (53)	13 (54)	13 (65)	0.65
Hyperlipidemia	20 (56)	12 (50)	9 (45)	0.22
Smoking	15 (42)	11 (46)	9 (45)	0.94
Obesity	9 (25)	5 (21)	7 (35)	0.55
Medications on admission				
Statin use	5 (14)	6 (25)	4 (20)	0.55
Beta-blocker use	5 (14)	4 (16)	4 (20)	0.44
ACE/ARB use	6 (16)	9 (38)	8 (40)	0.65
Aspirin	5 (14)	7 (29)	13 (65)	0.13
Reperfusion time, min	259 ± 201	—	—	—
Max CK, IU/l	1,942 ± 1,892	—	—	—
Max CK-MB, IU/l	186 ± 212	—	—	—
LVEF at the onset of MI, %	48 ± 17	—	—	—
Peak WBC counts, cells/μl	11,024 ± 2,720	—	—	—
Peak neutrophil counts, cells/μl	8,259 ± 2,621	—	—	—
Peak PBMC, cells/μl	679 ± 259	—	—	—

Data are expressed as mean ± SD or n (%).

ACE = angiotensin-converting enzyme; AMI = acute myocardial infarction; ARB = angiotensin receptor blocker; CK = creatine kinase; LAD = left anterior descending artery; LCX = left circumflex artery; LVEF = left ventricular ejection fraction; MB = myocardial band; PBMC = peripheral blood mononuclear cell; RCA = right coronary artery; SAP = stable angina pectoris; UAP = unstable angina pectoris; WBC = white blood cell.

plaque instability itself could affect monocyte dynamics even without necrosis. In UAP patients, we did not find any significant changes of the 2 monocyte subsets counts during the following 3 days (Figs. 4E and 4F). In accordance with previous studies (11), peak levels of plasma PlGF after AMI significantly correlated with peak monocyte counts ($r = 0.76$, $p < 0.001$). We also found that peak levels of PlGF after AMI significantly correlated with peak $CD14^+$

Table 2 Patient Characteristics and Peak Monocyte Subset Counts

	Peak Monocytes (/mm^2)	p Value	$CD14^+CD16^-$ Monocytes (/mm^2)	p Value	$CD14^+CD16^+$ Monocytes (/mm^2)	p Value
Age ≥70 yrs	654 ± 234	0.26	556 ± 248	0.32	65 ± 24	0.19
Age <70 yrs	739 ± 266		655 ± 251		77 ± 17	
Males, n	639 ± 174	0.79	567 ± 143	0.73	74 ± 39	0.79
Females, n	650 ± 262		607 ± 221		69 ± 25	
Cigarette smoking (+)	610 ± 177	0.37	582 ± 206	0.49	75 ± 22	0.29
Cigarette smoking (−)	689 ± 231		621 ± 192		63 ± 25	
Hypertension (+)	701 ± 190	0.5	644 ± 190	0.4	71 ± 20	0.26
Hypertension (−)	578 ± 231		534 ± 201		58 ± 25	
Diabetes mellitus (+)	745 ± 216	0.36	636 ± 224	0.63	73 ± 18	0.36
Diabetes mellitus (−)	617 ± 204		586 ± 189		62 ± 36	
Hyperlipemia (+)	663 ± 234	0.91	631 ± 157	0.52	72 ± 27	0.66
Hyperlipemia (−)	624 ± 199		547 ± 223		67 ± 16	
Anterior infarction (+)	699 ± 213	0.29	660 ± 193	0.15	78 ± 20	0.3
Anterior infarction (−)	584 ± 154		521 ± 172		64 ± 28	

Data are expressed as mean ± SD.

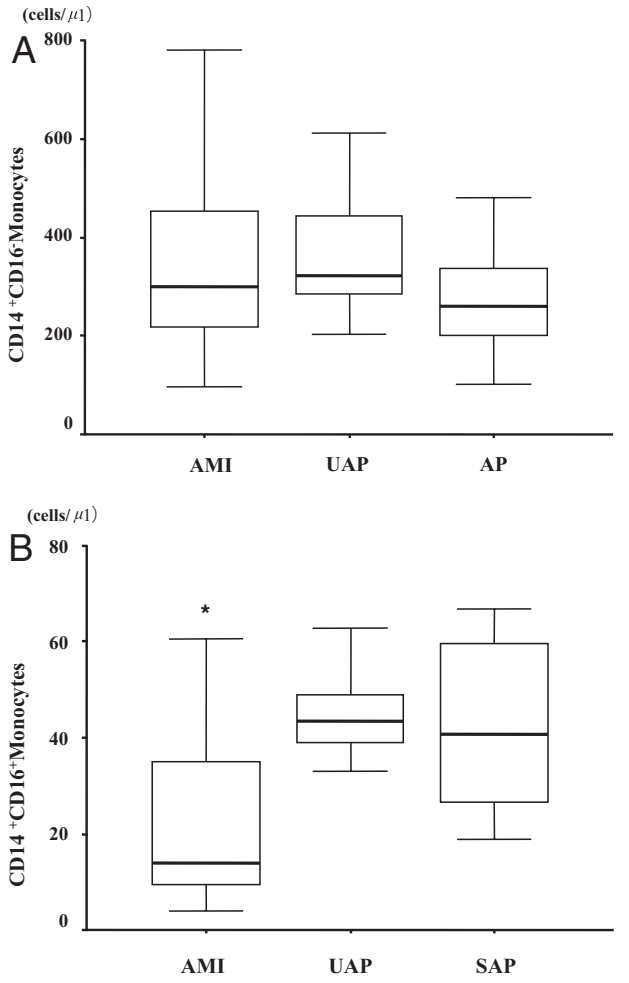

Figure 3 **Monocyte Subset Levels in Coronary Artery Disease**

Peripheral blood samples were obtained from patients with acute myocardial infarction (AMI) and unstable angina pectoris (UAP) as soon as possible after admission (day 1), and from patients with stable angina pectoris (SAP) on hospital day (day 1). Respective numbers of $CD14^+CD16^-$ monocytes **(A)**, and $CD14^+CD16^+$ monocytes **(B)** were determined in patients with AMI, UAP, and SAP. Data are represented as box plot with median and 25th to 75th percentiles **(boxes)** and 10th to 90th percentiles **(whiskers)**. *Value of $p < 0.01$ versus SAP.

$CD16^-$ monocyte counts ($r = 0.78$, $p < 0.001$), but not with peak $CD14^+CD16^+$ monocyte counts, suggesting that PlGF may be produced by these cells.

Relationship between peak CRP levels and peak monocyte subset levels. Peak $CD14^+CD16^-$ monocytes showed a significant positive correlation with peak CRP levels ($r = 0.62$, $p < 0.001$). However, peak $CD14^+CD16^+$ monocytes did not show any significant correlation with peak CRP levels. In addition, neither peak $CD14^+CD16^-$ monocytes nor $CD14^+CD16^+$ monocytes showed significant correlation with indicators of MI severity, such as peak CK, peak CK-myocardial band, and LVEF, suggesting that the increased numbers of the 2 distinct monocyte subsets do not simply reflect larger infarcts (data not shown).

Effects of 2 distinct monocyte subsets on acute phase myocardial salvage and chronic phase of LV function. Having demonstrated that $CD14^+CD16^-$ and $CD14^+CD16^+$ monocytes are sequentially mobilized from bone marrow into circulation, we next investigated the relationship between these 2 monocyte subset levels and the extent of myocardial salvage that occurred 7 days after AMI. The extent of myocardial salvage at 7 days after AMI was evaluated by CMR imaging as the difference between myocardium at risk (T2-weighted hyperintense lesion) and myocardial necrosis (delayed gadolinium enhancement) (Fig. 2). The peak levels of $CD14^+CD16^-$ monocytes were significantly negatively associated with the extent of myocardial salvage, whereas those of $CD14^+CD16^+$ monocytes showed no such significant association (Figs. 5A and 5B, respectively). Cine MRI imaging was performed in 30 patients (83%) during the chronic phase 6 months after the onset of AMI. In the 30 patients, LVEF increased, but not significantly, by $5 \pm 7\%$, from $47 \pm 10\%$ at baseline to $51 \pm 13\%$ at 6-month follow-up ($p = 0.098$). The peak levels of $CD14^+CD16^-$ monocytes were negatively correlated with the subsequent changes in LVEF observed during the chronic phase 6 months after the onset of AMI (ΔLVEF, $r = -0.60$, $p = 0.001$) (Fig. 5C), whereas those of $CD14^+CD16^+$ showed no significant association (data not shown).

Discussion

This study demonstrated for the first time that patients with ST-segment elevation AMI showed $CD14^+CD16^-$ and $CD14^+CD16^+$ monocytes that were sequentially mobilized after AMI successfully treated with PCI. More importantly, we showed for the first time that the peak levels of $CD14^+CD16^-$ monocytes, but not $CD14^+CD16^+$ monocytes, were significantly negatively associated with the extent of myocardial salvage that occurred 7 days after AMI. These results demonstrated that dynamic changes occur in 2 distinct monocyte subset levels in patients with AMI, and that stochastic profiling of this monocyte/macrophage system may hold clinical utility with respect to myocardial salvage after MI.

Several clinical studies have demonstrated that elevated monocyte counts are associated with LV dysfunction after PCI for AMI, suggesting a role for monocytes in the development of LV remodeling after reperfused MI (12,13). By contrast, Hojo et al. (14) reported that patients showing improved LV systolic function after MI exhibited significantly higher monocyte counts than did patients without improvement. Similarly, Iwama et al. (11) reported that increased monocyte counts associated with the local expression of PlGF were related to improved LV systolic function after MI.

Taking these findings together, it remains unclear how peripheral monocytosis is related to LV remodeling after successful PCI, and these contradicting results underscore the need to explore the relevance of monocyte heterogeneity

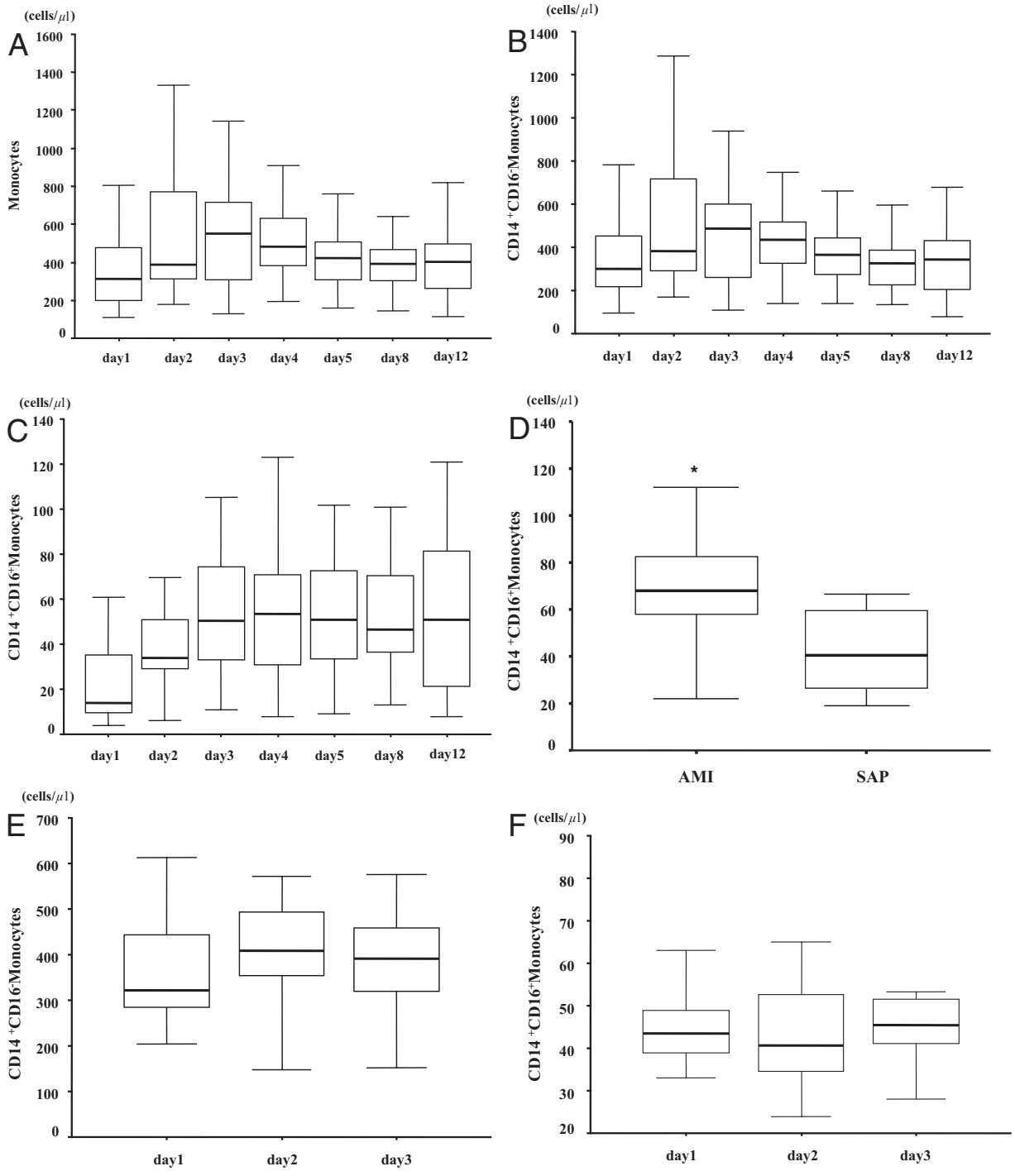

Figure 4 **Time Courses in Circulating Monocytes and Monocyte Subset Levels After AMI and UAP**

Respective numbers of **(A)** monocytes, **(B)** $CD14^+CD16^-$ monocytes, and **(C)** $CD14^+CD16^+$ monocytes were determined on days 1, 2, 3, 4, 5, 8, and 12 after acute myocardial infarction (AMI). **(D)** Next, individual peak values of $CD14^+CD16^+$ monocytes from patients with AMI were compared with those from patients with stable angina pectoris (SAP). Respective numbers of **(E)** $CD14^+CD16^-$ monocytes and **(F)** $CD14^+CD16^+$ monocytes were determined on days 1, 2, and 3 after admission in unstable angina pectoris (UAP) patients. Data are represented as box plot with median and 25th to 75th percentiles **(boxes)** and 10th to 90th percentiles **(whiskers)**. *Value of $p < 0.01$ versus SAP.

after AMI. In this regard, Nahrendorf et al. (5) have demonstrated that distinct monocyte subsets contribute in specific ways to myocardial ischemic injury in mouse MI. That is, Ly-$6C^{hi}$ monocytes, which correspond to $CD14^+CD16^-$ monocytes in humans, accumulate via CCR2, predominate at the site of injury during the first 3

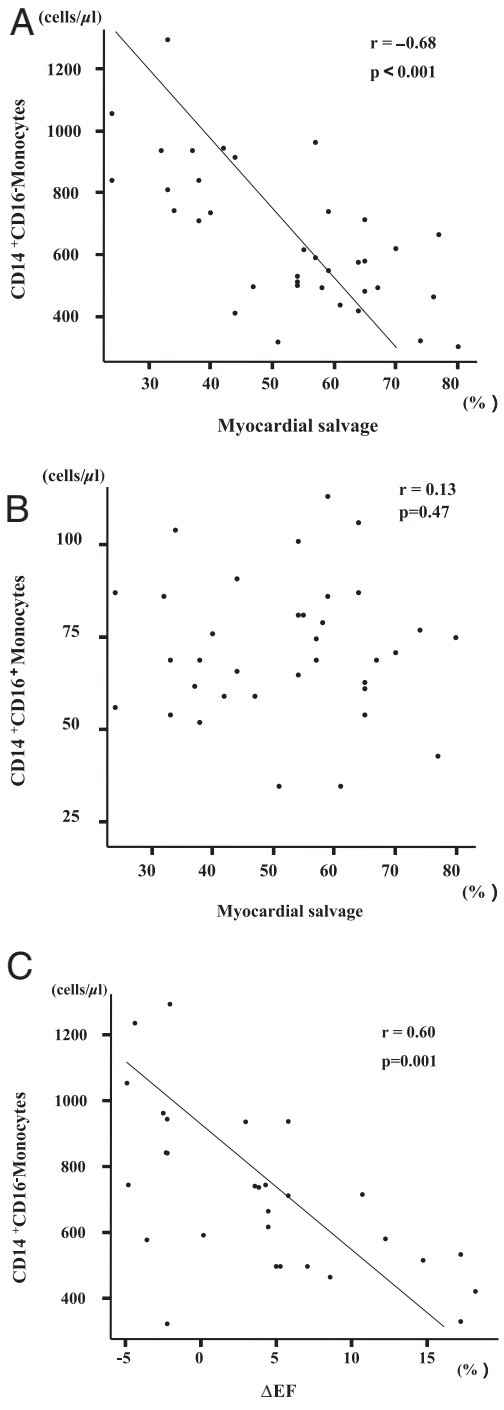

Figure 5 **Relationship Between 2 Monocyte Subset Levels and Extent of Myocardial Salvage**

The relationship between 2 distinct monocyte subset levels and extent of myocardial salvage during the acute phase or left ventricular ejection fraction (LVEF) during the chronic phase. Peak counts of **(A)** $CD14^+CD16^-$ monocytes but not **(B)** $CD14^+CD16^+$ monocytes significantly correlated with extent of myocardial salvage. Extent of myocardial salvage was demonstrated as percent salvaged myocardium (salvaged myocardium normalized to myocardium at risk). Left ventricle function was assessed with cine magnetic resonance imaging. **(C)** The peak levels of $CD14^+CD16^-$ monocytes were negatively correlated with the changes of LVEF (ΔEF) that occurred between the acute and chronic phases.

days, and scavenge necrotic debris by a combination of inflammatory mediator expression, proteolysis, and phagocytosis. Between 4 and 7 days after infarction, Ly-$6C^{lo}$ monocytes, which correspond to $CD14^+CD16^+$ monocytes in humans, accumulate preferentially via CX3CR1.

In accordance with the experimental study, we have demonstrated for the first time that 2 monocyte subsets, $CD14^+CD16^-$ and $CD14^+CD16^+$, are sequentially mobilized after AMI in the clinical settings. More importantly, we have also shown that the peak levels of $CD14^+CD16^-$ monocytes are significantly negatively correlated with myocardial salvage after AMI. However, the mechanisms through which $CD14^+CD16^-$ monocytes enhance injury remain unclear. Previous studies (15,16) have shown that monocyte chemoattractant protein (MCP)-1, a ligand for CCR2, is markedly up-regulated in an ischemic myocardium and is responsible for the recruitment of mononuclear cells into the injured myocardium. In addition, Dewald et al. (17) showed that $MCP^{-/-}$ mice have significantly lower tumor necrosis factor-α, interleukin-1β, and interleukin-6 messenger ribonucleic acid expression after 6 h of reperfusion compared with wild-type infarcts in a closed-chest model of reperfusion murine myocardial infarction. Taken together, monocytes recruited in the myocardium through CCR2/MCP-1 interactions might play a critical role in the pathogenesis of myocardial salvage. Moreover, in contrast to a previous experimental study, which shows that Ly-$6C^{lo}$ ($CD14^+CD16^+$ analogs) monocytes were found to be critical for myocardial healing via myofibroblasts accumulation, angiogenesis, and deposition of collagen, this study did not show any significant effect of $CD14^+CD16^+$ monocytes on myocardial salvage followed by reperfused MI. However, we could not exclude the possibility that it may potentially be the result of a short period of observation (7 days after reperfusion).

As a means of assessing the area at risk, Aletras et al. (7) have suggested T2-weighted CMR imaging, with the notable feature of decoupling the imaging for several days after the acute presentation. Furthermore, CMR imaging allows simultaneous direct visualization of not only myocardial necrosis by LE MRI but also the area at risk by T2-weighted MRI (8,9). Reperfusion leads to an inflammatory-like response with intracellular and extracellular myocardial edema (18), and subsequent prolongation of the T2 relaxation time and high T2 signal intensities (19). The high T2 signal intensity in AMI most likely reflects the increased free water content in the area of reversible injury (20,21). In fact, the area of high T2 signal abnormality closely matched the pathologically determined myocardial area at risk (18,22). Interestingly, Friedrich et al. (8) reported very recently that the area at risk can be visualized using T2-weighted CMR in patients with AMI. In contrast, LE is observed only in areas of irreversible myocardial injury (22). Thus, we can directly assess the extent of salvaged myocardium (T2 positive but LE negative) using the 2 methods.

Study limitations. First, the results were prospective in terms of patient enrollment but were observational in nature. Thus, our study does not provide a mechanistic explanation for the improvement of myocardial salvage that occurred 7 days after MI associated with the heterogeneity of monocyte subsets. Second, our study cannot determine whether the elevation of 2 distinct monocyte subsets reflects the extent of monocyte subset infiltration into an ischemic myocardium. Third, we did not perform analysis of peripheral monocytes, especially pro-inflammatory mediators by $CD14^+CD16^-$ cells; however, previous experimental work supports the inflammatory/injurious potential of the cells (15–17). Finally, although we performed CMR assessment of myocardial salvage 7 days after reperfusion, we cannot exclude the possibility that earlier acquisition would have influenced the extent of myocardial salvage.

Conclusions

In patients with primary AMI, $CD14^+CD16^-$ and $CD14^+CD16^+$ monocytes are sequentially mobilized after AMI. More importantly, the peak levels of $CD14^+CD16^-$ monocytes are associated with the impairment of myocardial salvage in the acute phase after AMI and adverse LV remodeling, indicating that manipulation of $CD14^+CD16^-$ monocytes could become a novel therapeutic target for salvaging ischemic damage.

Reprint requests and correspondence to: Dr. Toshio Imanishi, Department of Cardiovascular Medicine, Wakayama Medical University, 811-1, Kimiidera, Wakayama City, Wakayama 641-8510, Japan. E-mail: t-imani@wakayama-med.ac.jp.

REFERENCES

1. Geissmann F, Jung S, Littman DR. Blood monocytes consist of two principal subsets with distinct migratory properties. Immunity 2003; 19:71–82.
2. Gordon S, Taylor PR. Monocyte and macrophage heterogeneity. Nat Rev Immunol 2005;5:953–64.
3. Gordon S. Macrophage heterogeneity and tissue lipids. J Clin Invest 2007;117:89–93.
4. Libby P, Maroko PR, Bloor CM, Sobel BE, Braunwald E. Reduction of experimental myocardial infarct size by corticosteroid administration. J Clin Invest 1973;52:599–607.
5. Nahrendorf M, Swirski FK, Aikawa E, et al. The healing myocardium sequentially mobilizes two monocyte subsets with divergent and complementary functions. J Exp Med 2007;204:3037–47.
6. Kim RJ, Wu E, Rafael A, et al. The use of contrast-enhanced magnetic resonance imaging to identify reversible myocardial dysfunction. N Engl J Med 2000;343:1445–53.
7. Aletras AH, Tilak GS, Natanzon A, et al. Retrospective determination of the area at risk for reperfused acute myocardial infarction with T2weighted cardiac magnetic resonance imaging: histopathological and displacement encoding with stimulated echoes (DENSE) functional validation. Circulation 2006;113:1865–70.
8. Friedrich MG, Abedel-Aty H, Taylor A, Schulz-Menger J, Messroghli D, Dietz R. The salvaged area at risk in reperfused acute myocardial infarction as visualized by cardiovascular magnetic resonance. J Am Coll Cardiol 2008;51:1581–7.
9. Hirsch A, Nijveldt R, Haeck JDE, et al. Relation between the assessment of microvascular injury by cardiovascular magnetic resonance and coronary Doppler flow velocity measurements in patients with acute anterior wall myocardial infarction. J Am Coll Cardiol 2008;51:2230–8.
10. Ziegler-Heitbrock L. The CD14+CD16+ blood monocytes: their role in infection and inflammation. J Leukoc Biol 2007;81:584–92.
11. Iwama H, Uemura S, Naya N, et al. Cardiac expression of placental growth factor predicts the improvement of chronic phase left ventricular function in patients with acute myocardial infarction. J Am Coll Cardiol 2006;47:1559–67.
12. Jugdutt BI. Monocytosis and adverse left ventricular remodeling after reperfused myocardial infarction. J Am Coll Cardiol 2002;39:247–50.
13. Maekawa Y, Anzai T, Yoshikawa T, et al. Prognostic significance of peripheral monocytosis after reperfused acute myocardial infarction: a possible role for left ventricular remodeling. J Am Coll Cardiol 2002;39:241–6.
14. Hojo Y, Ikeda U, Zhu Y, et al. Expression of vascular endothelial growth factor in patients with acute myocardial infarction. J Am Coll Cardiol 2000;35:968–73.
15. Kakio T, Matsumori A, Ono K, Ito H, Matsushima K, Sasayama S. Roles and relationship of macrophage and monocyte chemotactic and activating factor/monocyte chemoattractant protein-1 in the ischemic and reperfused rat heart. Lab Invest 2000;80:1127–36.
16. Hayashidani S, Tsutsi H, Shiomi T, et al. Anti-monocyte chemoattractant protein-1 gene therapy attenuates left ventricular remodeling and failure after experimental myocardial infarction. Circulation 2003; 108:2134–40.
17. Dewald O, Zymek P, Winkelmann K, et al. CCL2/monocyte chemoattractant protein-1 regulates inflammatory responses critical to healing myocardial infarcts. Circ Res 2005;96:881–9.
18. Maxwell SR, Lip GY. Reperfusion injury: a review of the pathophysiology, clinical manifestations and therapeutic options. Int J Cardiol 1997;58:95–117.
19. Wisenberg G, Prato FS, Carroll SE, Turner KL, Marshall T. Serial nuclear magnetic resonance imaging of acute myocardial infarction with and without reperfusion. Am Heart J 1988;115:510–8.
20. Bouchard A, Reeves RC, Cranney G, Bishop SP, Pohost GM. Assessment of myocardial infarct size by means of T2-weighted 1H nuclear magnetic resonance imaging. Am Heart J 1989;117:281–9.
21. Scholz TD, Martins JB, Skorton DJ. NMR relaxation times in acute myocardial infarction: relative influence of changes in tissue water and fat content. Magn Reson Med 1992;23:89–95.
22. Garcia-Dorado D, Oliveras J, Gili J, et al. Analysis of myocardial oedema by magnetic resonance imaging early after coronary artery occlusion with or without reperfusion. Cardiovasc Res 1993;27: 1462–9.

Key Words: chemokine ■ monocyte ■ myocardial salvage ■ acute myocardial infarction.